J Therm Anal Calorim (2016) 126:1281–1288
DOI 10.1007/s10973-016-5601-9

Morphology and dynamic mechanical properties of long glass fiber-reinforced polyamide 6 composites

Mei Hua Liu[1] · Rui Li[1] · Guo Wang[2] · Ze Yun Hou[1] · Bin Huang[1]

Received: 28 January 2016 / Accepted: 30 May 2016 / Published online: 21 June 2016

Abstract Long glass fiber-reinforced polyamide 6 (LGF–PA6) composites were prepared by using self-designed impregnation device. Polypropylene grafted with maleic anhydride (PP-g-MAH) and polyolefin elastomer grafted with maleic anhydride (POE-g-MAH) were chosen as compatibilizers. Dynamic mechanical properties of LGF–PA6 composites were investigated by using dynamic mechanical analysis (DMA). The DMA measurement results showed that test frequency, long glass fiber content and compatibilizers had an influence on dynamic mechanical properties and glass transition temperature (T_g) of LGF–PA6 composites. The frequency had a complex influence on storage modulus (E'), loss modulus (E'') and loss tangent (tan δ). The T_g of the composites is shifted to high temperature with the increasing of test frequency and was affected insignificantly by the glass fiber content. Storage modulus and loss modulus (E'') increased with the increasing fiber content, while the tan δ decreased. The effect of the addition of PP-g-MAH and POE-g-MAH on the dynamic mechanical properties of LGF–PA6 composites was complex. Scanning electron microscopy (SEM) was used to investigate the morphology of the fractured composites surface. The SEM results suggested that the PP-g-MAH and POE-g-MAH both improved the fiber/matrix interface adhesion, which was consistent with the DMA measurement results.

✉ Mei Hua Liu
liumeihua@csu.edu.cn

[1] School of Materials Science and Engineering, Central South University, Changsha, China

[2] Wuhan Sunwill Saitec Engineering Plastics Co., Ltd., Wuhan, China

Keywords Long glass fiber · Polyamide 6 · Compatibilizer · DMA

Introduction

Long glass fiber-reinforced thermoplastic composites used in semi-structural and engineering applications have grown dramatically in the past decades, due to their lightweight, high properties, good processability and recyclability [1–4]. Long glass fiber-reinforced polyamide 6 (LGF–PA6) composites are excellent composites in terms of their high comprehensive properties and temperature resistance. Many researchers pay attention to the effect of variables such as the fiber length, content, diameter, orientation and sizing on the mechanical properties of LGF–PA6 composites [5–11].

Viscoelasticity is one of the important parameters to characterize the processing and usability of the materials. The composites make the relationship between structure and performance of the materials more complex due to the formation of interface. Dynamic mechanical analysis (DMA) is one of practical and sensitive instruments to study the viscoelastic behavior of materials, and it allows for a quick and easy measurement of material properties, such as storage modulus (E'), loss modulus (E'') and loss tangent (tan δ), under periodic stress. It can provide more useful information on the molecular chain structure and the interface between glass fiber and PA6 matrix. That is to say, DMA can provide more information on mechanical relaxation and the interaction between phase boundary layers. The dynamic mechanical properties of materials can provide information on the end-user performance and are key to guarantee the service performance, especially for the critical application of the product, thereby building up the user confidence in potential application. The dynamic

mechanical properties of composites depend on fiber content, fiber orientation, interface between fiber/matrix and the mode of testing [12–14]. There have been lots of dynamic mechanical properties of fiber-reinforced polymer composites [12–18]. Sarkhel et al. [19] found that there was a notable increase in stiffness of the PE-EPDM matrix as a result of jute fiber reinforcement, and the tan δ of composites is treated with compatibilizer shown lower magnitude as compared to untreated composites. He et al. [20] found that the glass fiber transition temperature of PPESK/silica composites was significantly enhanced as the SiO_2 content was increased, the damping peaks of composites increased and shifted to higher temperature with increasing of SiO_2 content; the damping peaks of composites shifted to higher temperature with increasing of testing frequency. Zuo et al. [21] applied DMA to the aging study of the pure and stabilized LGF–PA6 composites. However, so far, few systematic DMA studies on LGF–PA6 composites have been reported.

In this article, LGF–PA6 composites were prepared by a self-designed device. PP-g-MAH and POE-g-MAH were selected as compatibilizers. We studied the frequency, glass fiber content and compatibilizers on the dynamic mechanical properties of the LGF–PA6 composites.

Experimental

Materials

A commercially available polyamide 6, YH 400, was purchased from Yueyang Petrochemical, with the melt flow rate (MFR) of 22 g/10 min. Glass fibers, EDR17-2400-362J, supplied by Jushi Group Co., Ltd., were used as reinforcement material for LGF–PA6 composites. The glass fibers were treated with silane coupling agent by the supplier before purchase. PP-g-MAH and POE-g-MAH were supplied by Ningbo Nengzhiguang New Materials Technology Co., Ltd. The mass ratio of the resin matrix and the compatibilizer was 90/10. The antioxidant 1098 was purchased from BASF group. The mass ratio of the antioxidant and the composite was 0.3/100.

Sample preparation

LGF–PA6 composites with different glass fiber contents were produced by an extrusion–impregnation device. The coating twin-screw extruder (TDS-35B, Nanjing Norda Xinye Extrusion Equipment Co., Ltd., China) was connected with an impregnation device by a joint. The process is shown schematically in Fig. 1. The temperature of the extruder was set at 210–230–240–260 °C from hopper to die, and the screw speed was 100 rpm. The temperature of the joint and the impregnation groove were set at 270 and 300 °C, respectively. The temperature of device for preheating glass fiber was set at 100 °C. The PA6 resin and the addition agent, mixed earlier, were melted in the extruder and then squeezed into the impregnation groove, in where the glass fibers were wetted by the PA6 melt. After cooling, the continuous strands were chopped into pellets of 12 mm length for injection molding.

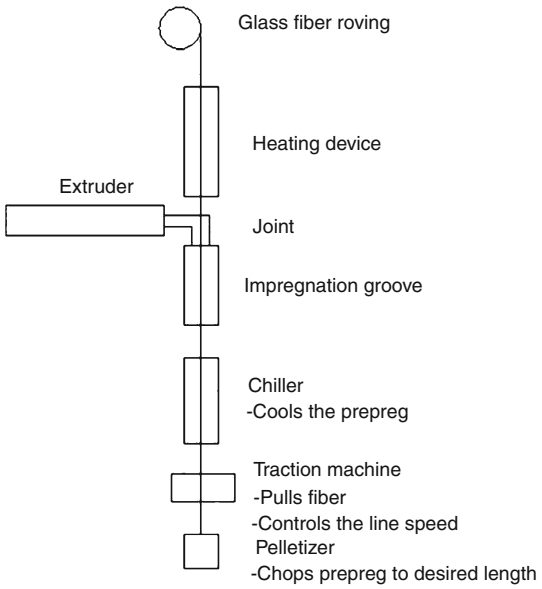

Fig. 1 Schematic diagram of the process

Injection molding

The LGF-PA6 pellets were molded into test bars on a Yizumi molding machine (UN90SK, Guangdong Yizumi Precision Machinery Co., Ltd., China). The temperatures were 230–235–240–245 °C from hopper to die, and the mold temperature was 60 °C. The injection pressure was set at 110 MPa. The flow rate was 30 %.

Dynamical mechanical analysis (DMA)

A dynamic mechanical analyzer (Q800, TA instruments, USA) was employed to carry out DMA experiments in signal cantilever mode. All the calibrations (position, force, clamp mass) were done according to the manufacture's recommendations. The measurements were taken at 2, 5, 8, 10 and 15 Hz, respectively. The temperature was controlled from 27 to 200 °C at a ramp rate of 3 °C min^{-1} under a N_2 flow rate of 40 mL min^{-1}.

Scanning electron microscopy (SEM)

The samples were cryogenically fractured in liquid nitrogen by bending the samples perpendicular to the shear flow

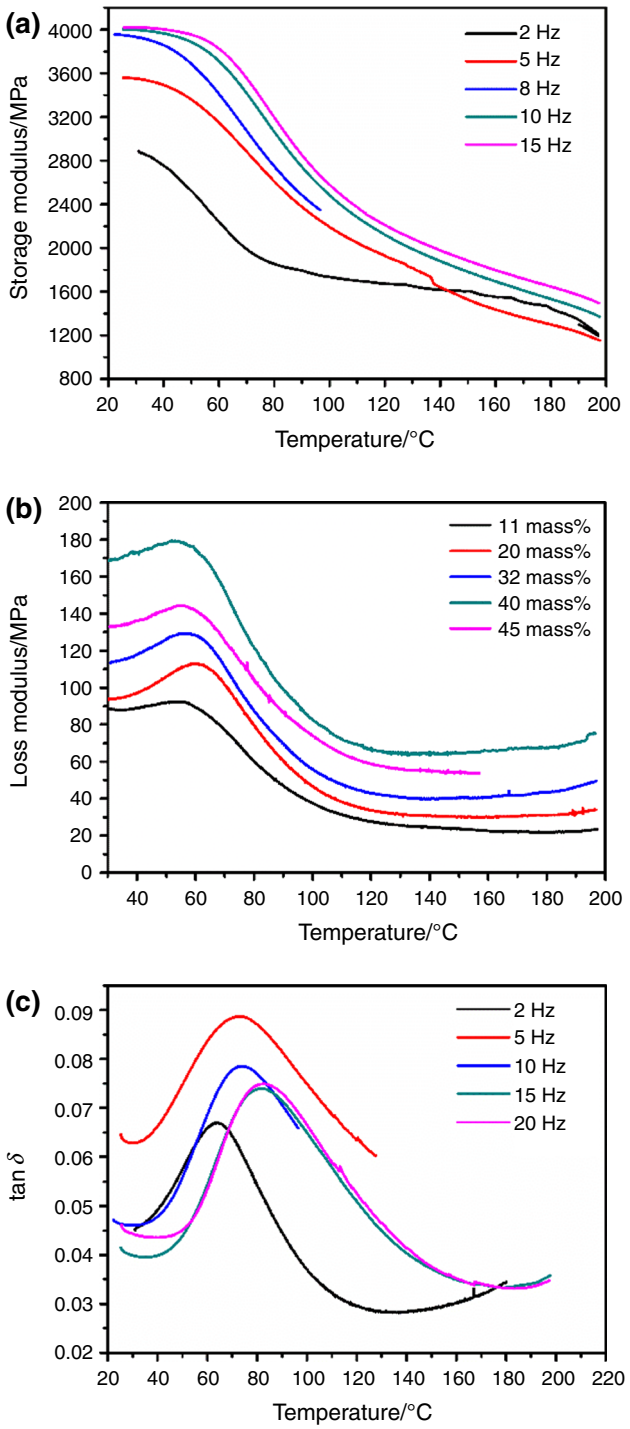

Fig. 2 Effect of test frequency on dynamic mechanical properties versus temperature. **a** Storage modulus, **b** loss modulus, **c** tan δ

direction. The fractured surface of samples was coated with a gold layer before examination, and the microstructural analysis was studied using a scanning electron microscope instrument (Quanta 200, FEI, USA).

Table 1 Results of DMA of the LGF (32 mass%)–PA6 composites at different test frequencies

Frequency/Hz	Loss modulus/MPa E''_{max}	Loss tangent tan δ_{max}	Temperature/°C	
			E''_{max}	tan δ_{max}
2	129.3	0.06698	54.9	63.0
5	263.6	0.0887	61.1	72.2
8	241.5	0.0785	66.8	74.3
10	233.4	0.07396	74.4	81.9
15	244.3	0.07490	74.5	82.5

Results and discussion

Dynamic mechanical properties

Influence of the test frequency

The test frequencies play a significant role in dynamic mechanical properties of the composites. Figure 2 shows the effect of test frequencies on the dynamic mechanical properties of LGF (32 mass%)–PA6 composites. Table 1 shows the E''_{max} and tan δ_{max} values and their corresponding temperatures of the LGF (32 mass%)–PA6 composites at different test frequencies. The glass transition temperature, T_g, is defined as the temperature at the maximum peak on the energy dissipation curve or loss modulus curve.

Figure 2a shows the variation of the storage modulus of the composites with temperature at different test frequencies. The storage modulus of the composites increases gradually with increasing the test frequency. Under a constant stress, composites undergo a decrease in their elastic modulus due to the molecule chains of polymer matrix rearrangement in order to minimize the localized stresses. The storage modulus of the composites decreases with time goes, so the modulus of composites at 15 Hz is higher than that at 2 Hz. It is also clear that the storage modulus of the composites decreases dramatically with increasing the temperature, as shown in Fig. 2a. The reason is that the viscoelasticity properties of polymer matrix are the functions of temperature, time and frequency [16, 17]. It is obvious that the LGF (32 mass%)–PA6 composite displays a high storage modulus at the temperature range of 20–40 °C. The reason is that, at this temperature, LGF–PA6 composites are in glassy state, and the majority of chain segments are frozen. In the range of 40–100 °C, glassy–rubbery transition, a dramatic drop appears in storage modulus of the LGF (32 mass%)–PA6 composites, which results from the motion of polymer chain segments in the free volume. At this temperature range, the

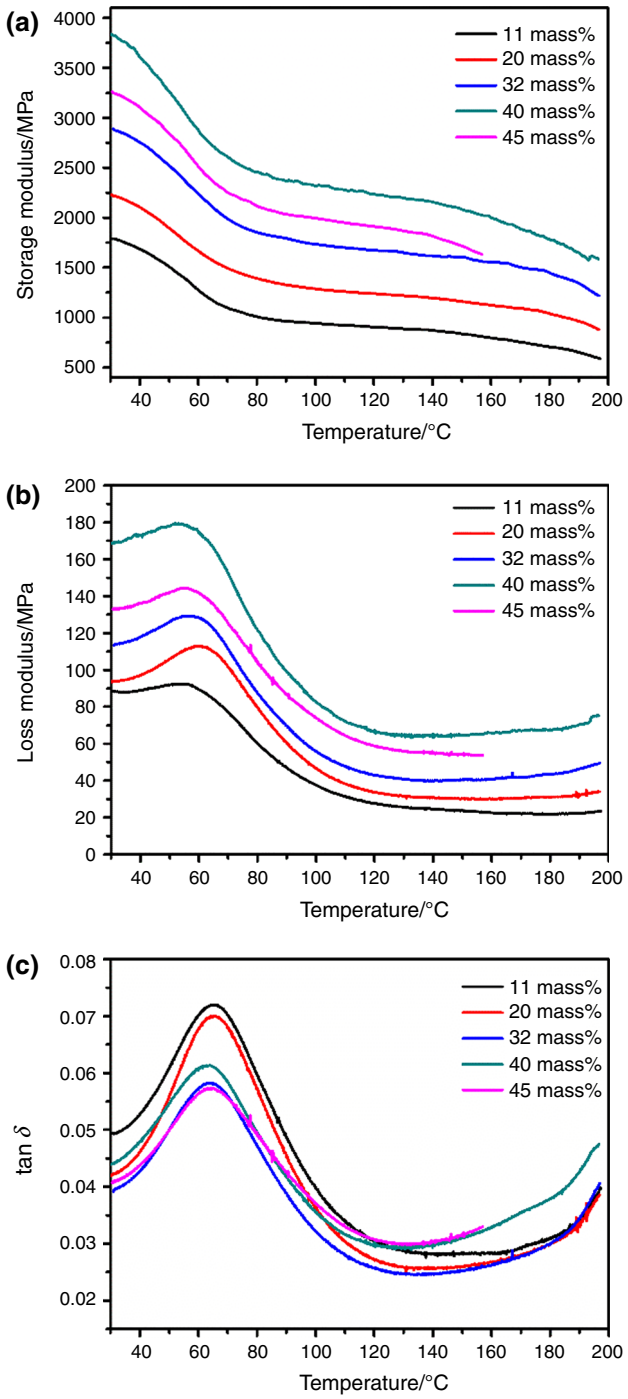

Fig. 3 Effect of fiber content on dynamic mechanical properties versus temperature. **a** Storage modulus, **b** loss modulus, **c** tan δ

composites are neither glassy nor rubbery-like. Finally, over the range of 100–200 °C, the glassy state turns to rubbery state, which is relevant to long-range motion of the chain segments that leads to softness of the materials. The storage modulus of the LGF (32 mass%)–PA6 composites in the rubbery state is relatively low.

Table 2 Results of DMA of the LGF–PA6 composites with different fiber contents

Fiber content/ mass%	Loss modulus/MPa	Loss tangent	Temperature/ °C	
	E''_{max}	tan δ_{max}	E''_{max}	tan δ_{max}
11	92.5	0.07205	56.7	65.4
20	113.0	0.07007	59.6	65.6
32	129.3	0.06699	54.9	63.0
40	179.2	0.06135	53.5	62.94
45	144.4	0.05735	55.5	63.04

Figure 2b shows the effect of test frequencies on the loss modulus of LGF (32 mass%)–PA6 composites with temperature. The loss modulus increases with the increasing frequency, and the α-relaxation peak of polymer matrix shifts toward higher-temperature region with the increasing of test frequency.

The ratio of loss modulus to storage modulus is measured as the mechanical loss tangent (tan δ). The variation of tan δ as a function of temperature at different frequencies is shown in Fig. 2c. The influence of frequency on the tan δ is complex. At low frequency, the chain motion can keep up with the change of the external force, and the internal friction is low; therefore, the tan δ is low. With the increasing frequency, the internal friction begins to increase because the chain motion falls behind the external force; therefore, the tan δ increases. When the frequency increases to 8 Hz, the chain motion does not keep up with the changes of the external force completely and the internal friction becomes slow, which results in the drop of tan δ. And the α-relaxation peak of composites is shifted toward higher-temperature region with the increasing frequency. It can be seen in Fig. 2b, c and Table 1 that the peak temperatures of tan δ and loss modulus show that the glass transition shifts to higher temperatures as the test frequency increases, which is due to the increasing speed of the molecule motion. The T_g value indicated by the tan δ_{max} peak is higher than that indicated from the corresponding E''_{max} peak as given in Table 1.

Influence of the glass fiber content

Figure 3 shows the effect of glass fiber content on the storage modulus, loss modulus and tan δ as a function of temperature of LGF–PA6 composites at 2 Hz. Table 2 shows the E''_{max} and tan δ_{max} values and their corresponding temperatures of the LGF–PA6 composites with different glass fiber contents. The glass fiber content has a significant effect on the dynamical mechanical properties as shown in Fig. 3. The storage modulus of the composites gradually increases with increasing glass fiber content, due to the

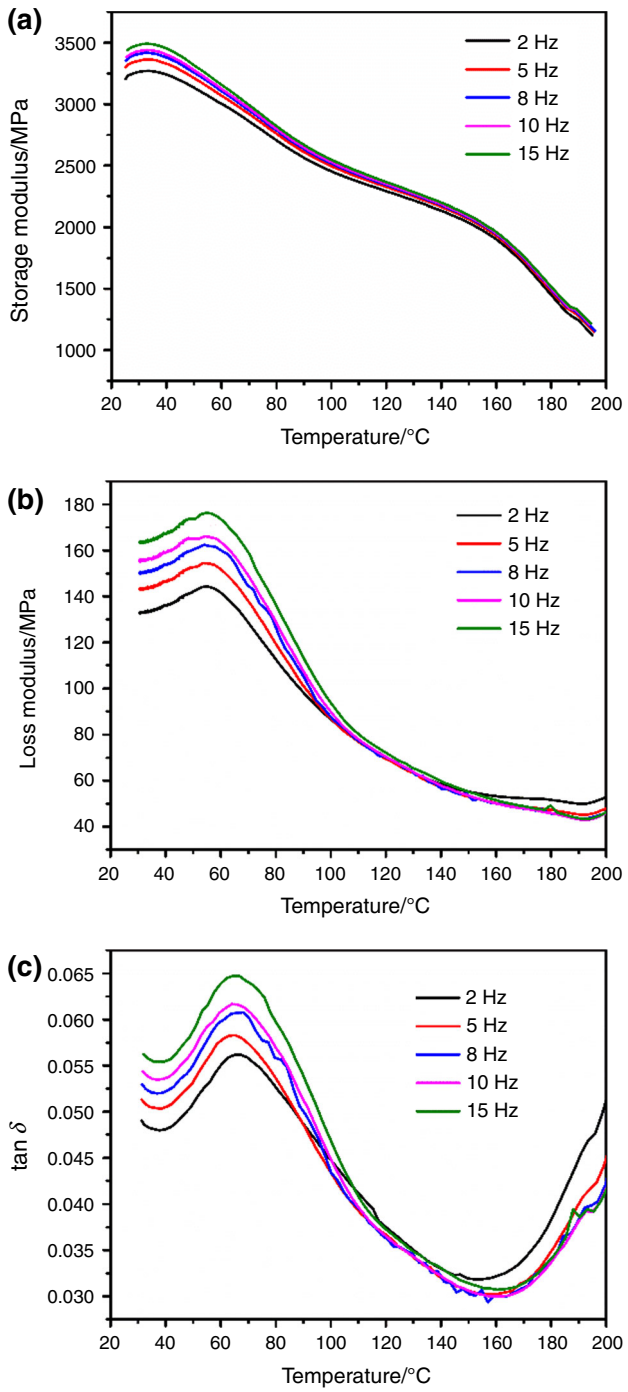

Fig. 4 Effect of PP-g-MAH on dynamic mechanical properties versus temperature. **a** Storage modulus, **b** loss modulus, **c** tan δ

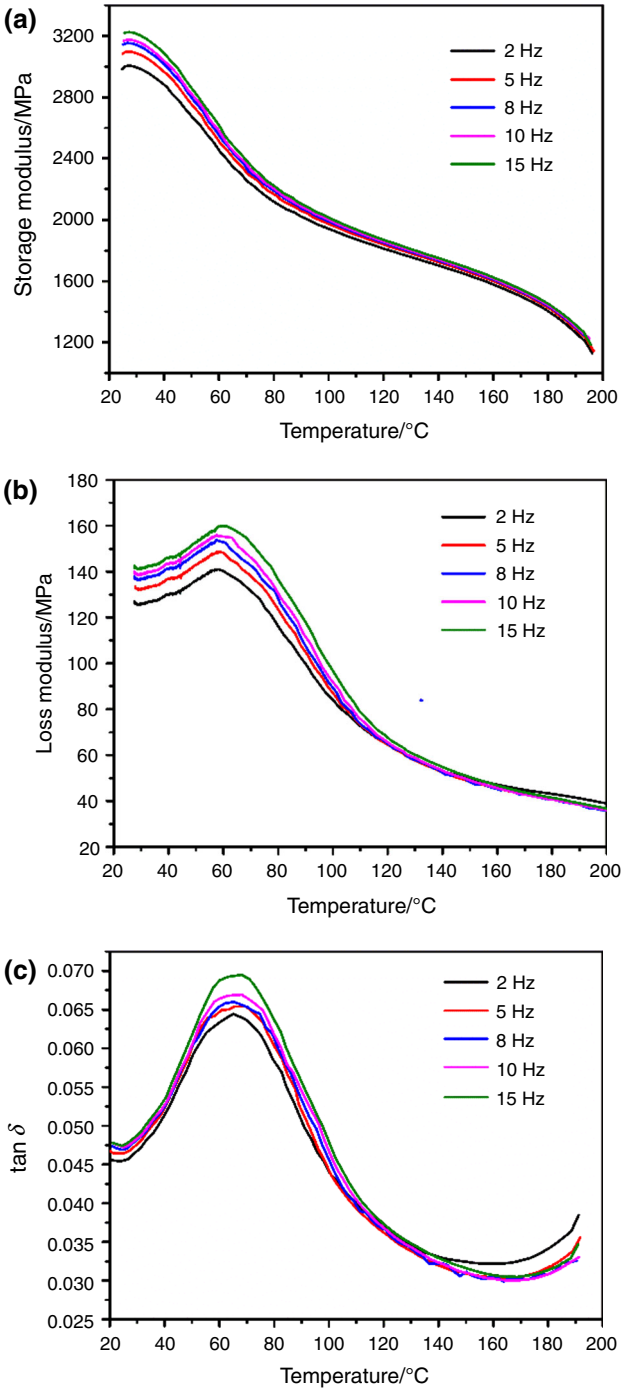

Fig. 5 Effect of POE-g-MAH on dynamic mechanical properties versus temperature. **a** Storage modulus, **b** loss modulus, **c** tan δ

increase in stiffness of the matrix with the reinforcement effect imparted by the fibers that allow greater stress transfer at interface [12, 16, 22], except for the LGF (45 mass%)–PA6 composites, for which a drop of about 10 % is observed. The reinforcing efficiency of composite depends not only on glass fiber content, but also on the degree of the long glass fiber dispersion and its length; the observed decline is a sequence of the deterioration of these parameters as a consequence of the increasing glass fiber content. The loss modulus of the composites gradually increases with increasing glass fiber content, too, maybe due to the fact that the addition of fiber restricts the chain segments motion, except for the LGF (45 mass%)–PA6 composites. The tan δ decreases gradually with increasing the glass fiber content. The reinforcing fibers restrict the mobility of the polymer chains, raise the storage modulus

Table 3 Results of DMA of the LGF–PA6 composites with different compatibilizers

Sample	Loss modulus/MPa	Loss tangent	Temperature/°C	
	E''_{max}	tan δ_{max}	E''_{max}	tan δ_{max}
LGF–PA6	129.3	0.06699	54.9	63.0
LGF–PA6/PP-g-MAH	144.4	0.05736	54.0	65.0
LGF–PA6/POE-g-MAH	141.0	0.06446	58.3	64.6

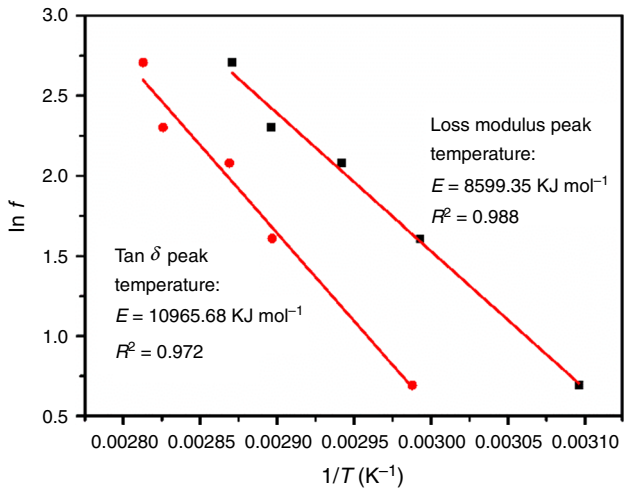

Fig. 6 Plot of the ln f versus $1/T_g$

values and reduce the viscoelastic lag between the stress and the strain, and hence, the tan δ value is decreased in the composites with the increasing glass fiber content. In the range of 11–45 mass% glass fiber content, the T_g of the composite indicated by the tan δ_{max} peak and loss modulus peek both hardly affected by the glass fiber as shown in Fig. 3c and Table 2.

Influence of compatibilizers

Figures 4 and 5 show the effect of PP-g-MAH and POE-g-MAH on the storage modulus, loss modulus and tan δ as a function of temperature of LGF/PA6 composites with 32 mass% long glass fiber, respectively. Table 3 shows the E''_{max} and tan δ_{max} values and their corresponding temperatures of the three composites at 2 Hz. The addition of PP-g-MAH and POE-g-MAH both increases the storage modulus of LGF–PA6 composites and decreases the loss modulus and tan δ of LGF–PA6 composites. The addition of PP-g-MAH gives a higher increase in storage modulus and decrease in tan δ than that of the addition of POE-g-MAH, due to the fact that PP-g-MAH gives a better interface adhesion between fiber and matrix that can transfer stress on interface better. This result interprets that the poor interfacial bonding between fiber and matrix tends to dissipate more energy and shows high magnitude of tan δ in comparison with the strongly bonded interface. From Figs. 4 and 5 and Table 3, it is clear that the T_g of the composites shifts to higher temperatures. And the PP-g-MAH gives a higher increase in T_g and lower tan δ, which indicates that the LGF–PA6/PP-g-MAH composites have a stronger interface strength than LGF–PA6/POE-g-MAH composites. This change is attributed to the decrease in the chain motion beyond the interface. The trend in glass transition temperatures from the tan δ is in agreement with those determined from loss modulus.

However, from Figs. 4 and 5, it is clear that the effect of testing frequency on the dynamic mechanical properties of LGF–PA6/PP-g-MAH and LGF–PA6/POE-g-MAH composites is different from that on LGF/PA6 composites. All of the storage modulus, loss modulus and tan δ of LGF–PA6/PP-g-MAH and LGF–PA6/POE-g-MAH composites increase gradually with increasing the test frequency, which indicates that the addition of compatibilizers reduces the sensitivity of dynamic mechanical properties of LGF–PA6 composites to test frequency.

Calculation of the activation energy

It is obvious that storage modulus, loss modulus and α-relaxation show strong frequency dependency as shown in Fig. 2. Loss modulus peak and tan δ peak are shifted to high-temperature zones with increasing frequency, and the shift of the two peaks shows strong regularity. The apparent activation energy (ΔE_α) for glass transition can be used to characterize the relationship between the shift of T_g and frequency. The Arrhenius equation (especially over a limited frequency range) is adopted to connect with this interrelationship for calculating the activation energy of α-relaxation [23]. The activation energies of α-relaxation are determined based on Eq. (1).

$$\Delta E_\alpha = -R\left[\frac{\mathrm{d}\ln f}{\mathrm{d}1/T_g}\right] \quad (1)$$

where R is gas constant, f is the test frequency and T_g is corresponding α-relaxation temperature.

A series of f and T_g are obtained from the multi-frequency DMA measurements, and the plot of ln f versus 1/

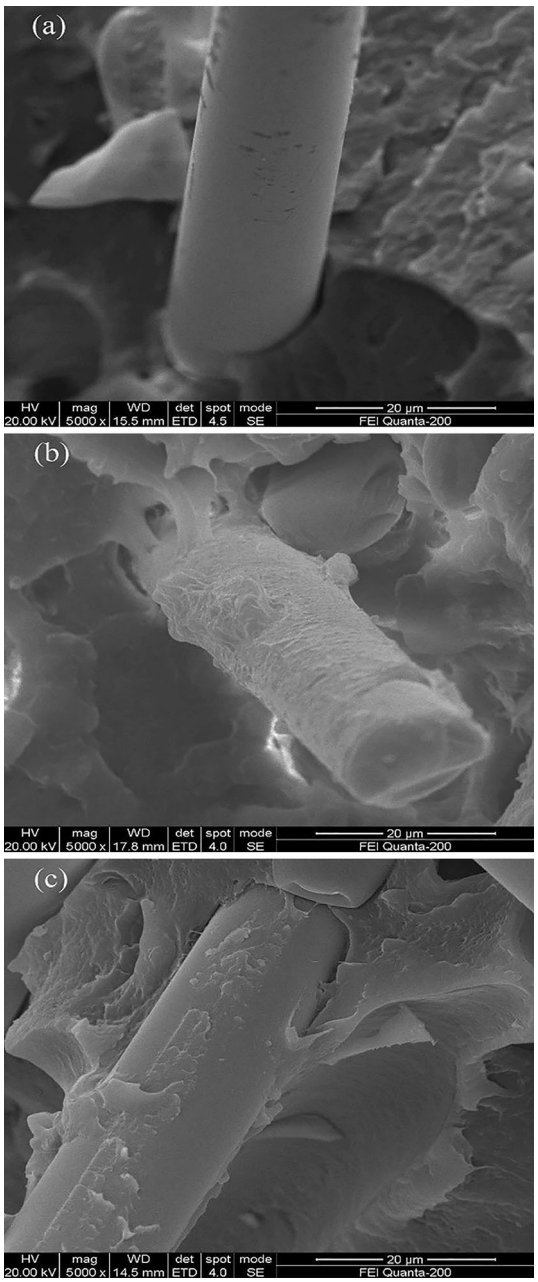

Fig. 7 SEM graphs of **a** LGF–PA6, **b** LGF–PA6/PP-g-MAH, **c** LGF–PA6/POE-g-MAH

T_g is shown in Fig. 6. According to the equation, the plot of ln f versus $1/T_g$ should give a straight line with a slope that is proportional to ΔE_α of the composites. Ln f against $1/T_g$ has a good linear correlation as shown in Fig. 6, and ΔE_α is calculated from the value of the slope. As a result, ΔE_α of LGF–PA6 composites based on the loss modulus peak temperature and tan δ peak temperature are 8599.4 and 10,965.7 kJ mol^{-1}, respectively.

Fractographic analysis

The SEM photographs of the fractured surfaces of LGF–PA6, LGF–PA6/PP-g-MAH and LGF–PA6/POE-g-MAH composites are shown in Fig. 7. As we all know, glass fiber-reinforced composites absorb energy via three major mechanisms: fiber breakage, fiber pull-out and matrix crack propagation. The glass fibers of LGF–PA6 composites are shown in Fig. 7a. The surface of the long glass fiber is clear and smooth, which indicates that there is a poor interface between fiber/matrix. It should be noted that a fiber that is not bound to the polymer matrix is much more likely to pull out during fracture, as opposed to breaking off at the fracture surface, thereby making them more visible. The glass fiber of LGF–PA6/PP-g-MAH composites is coated in a sheath of the polymer blend that comprises the matrix as shown in Fig. 7b. The interfacial adhesion between glass fiber and resin matrix is better than LGF–PA6 composites. The surface of long glass fiber of LGF–PA6/POE-g-MAH composites is coated with a thin layer of PA6 matrix, as shown in Fig. 7c. The morphology of the three different composites is in consistent with the dynamic mechanical properties discussed above.

Conclusions

The storage modulus and glass transition temperature of the composites both increase with the amplifying test frequency. The loss modulus and tan δ both increase at first and then decrease with the amplifying test frequency. The glass transition temperature of LGF–PA6 composites shifts to higher temperature with the amplifying test frequency. Both of storage modulus and loss modulus increase with the increasing glass fiber content; however, the tan δ is reverse. The glass transition temperature of LGF–PA6 composites decreases slightly with the increasing glass fiber content. The addition of PP-g-MAH and POE-g-MAH both increases the storage modulus and loss modulus, decreases the tan δ, and shifts the glass transition temperature to higher temperature at 2 Hz; however, the addition of these two compatibilizers reduces the sensitivity of dynamic mechanical properties of LGF–PA6 to test frequency. According to an Arrhenius equation, the ΔE_α of LGF–PA6 composites at the α-relaxation based on the loss modulus peak temperature and tan δ peak temperature are 8599.4 and 10,965.7 kJ mol^{-1}, respectively.

SEM result reveals that the addition of PP-g-MAH and POE-g-MAH improves the fiber/matrix interface adhesion.

References

1. Wang JC, Geng CZ, Luo F, Liu YM, Wang K, Fu Q, He BB. Shear induced fiber orientation, fiber breakage and matrix molecular orientation in long glass fiber reinforced polypropylene composites. Mater Sci Eng. 2011;528:3169–76.
2. Arao Y, Yumitori S, Suzuki H, Tannka T, Tannka K, Katayama T. Mechanical properties of injection-molded carbon fiber/polypropylene composites hybridized with nanofillers. Compos Part A Appl. 2013;55:19–26.
3. Köckritz T, Schiefer T, Jansen I, Beyer E. Improving the bond strength at hybrid-yarn textile thermoplastic composites for high-technology applications by laser radiation. Int J Adhes Adhes. 2013;46:85–94.
4. Lee DW, Ma SW, Lee KY. Electrical and mechanical properties of carbon/glass hybridized reinforced polypropylene composites. Macromol Res. 2013;21:767–74.
5. Thomason JL. The influence of fiber length, diameter and concentration on the modulus of glass fiber reinforced polyamide 6,6. Compos Part A Appl. 2008;39:1732–8.
6. Thomason JL. The influence of fiber length, diameter and concentration on the strength and strain to failure of glass fiber-reinforced polyamide 6,6. Compos Part A Appl. 2008;39:1618–24.
7. Thomason JL. The influence of fibre length, diameter and concentration on the impact performance of long glass-fiber reinforced polyamide 6,6. Compos Part A Appl. 2009;40:114–24.
8. Ozkoc G, Bayram G, Bayramli E. Effects of polyamide 6 incorporation to the short glass fiber reinforced ABS composites: an interfacial approach. Polymer. 2004;45:8957–66.
9. Laura DM, Keskkula H, Barlow JW, Paul DR. Effect of glass fiber surface chemistry on the mechanical properties of glass fiber reinforced, rubber-toughened nylon 6. Polymer. 2002;43:4673–87.
10. Laura DM, Keskkula H, Barlow JW, Paul DR. Effect of glass fiber and maleated ethylene–propylene rubber content on tensile and impact properties of nylon 6. Polymer. 2000;41:7165–74.
11. Laura DM, Keskkula H, Barlow JW, Paul DR. Effect of glass fiber and maleated ethylene–propylene rubber content on the impact fracture parameters of nylon 6. Polymer. 2001;42:6161–72.
12. Ray D, Sarkar BK, Das S, Rana AK. Dynamic mechanical and thermal analysis of vinylester-resin-matrix composites reinforced with untreated and alkali-treated jute fibers. Compos Sci Technol. 2002;62:911–7.
13. Cucos A, Budrugeac P, Miu L. DMA and DSC studies of accelerated aged parchment and vegetable-tanned leather samples. Thermochim Acta. 2014;583:86–93.
14. Mancic L, Osman RFM, Costa AMLM, d'Almeida JRM, Marinkovic BA, Rizzo FC. Thermal and mechanical properties of polyamide 11 based composites reinforced with surface modified titanate nanotubes. Mater Des. 2015;83:459–67.
15. Vilas JL, Laza JM, Garay MT, Rodri M. Unsaturated polyester resins cure: kinetic, rheologic, and mechanical dynamical analysis. II. The glass transition in the mechanical dynamical spectrum of polyester networks. J Polym Sci. 2001;39:146–52.
16. He M, Zhang DH, Guo JB, Qin SH, Ming XX. Mechanical, thermal, and dynamic mechanical properties of long glass fiber-reinforced thermoplastic polyurethane/polyoxymethylene composites. Polym Compos. 2014;35:2067–73.
17. Liu MH, Hou HY, Peng HJ, Li M. The influence of the active diluents cyclohexene oxide on the curing processing. J Therm Anal Calorim. 2015;122:509–15.
18. Wong DTH, Williams HL. Dynamic mechanical and vibration damping properties of polyurethane compositions. J Appl Polym Sci. 1983;28:2187–207.
19. Sarkhel G, Choudhury A. Dynamic mechanical and thermal properties of PE-EPDM based jute fiber composites. J Appl Polym Sci. 2008;26:3442–53.
20. He W, Xing T, Liao GX, Lin W, Deng F, Jian XJ. Dynamic mechanical properties of PPESK/silica hybrid materials. Polym Plast Technol Eng. 2009;48:164–9.
21. Zuo XL, Zhang KZ, Lei Y, Qin SH, Hao Z, Guo JB. Influence of thermooxidative aging on the static and dynamic mechanical properties of long-glass-fiber-reinforced polyamide 6 composites. J Appl Polym Sci. 2014;131:1082–90.
22. Hameed N, Sreekumar PA, Francis B, Yang WM, Thomas S. Morphology, dynamic mechanical and thermal studies on poly(-styrene-co-acrylonitrile) modified epoxy resin/glass fiber composites. Compos Part A Appl. 2007;38:2422–32.
23. Li C, Fan H, Hu J, Li B. Novel silicone aliphatic amine curing agent for epoxy resin: 1, 3-Bis (2-aminoethylaminomethyl) tetramethyldisiloxane. 2. Isothermal cure, and dynamic mechanical property. Thermochim Acta. 2012;549:132–9.